iMRI 2025;29(4):216-224
https://doi.org/10.13104/imri.2025.0025
eISSN 2384-1109

Original Article

Received: June 5, 2025
Revised: October 27, 2025
Accepted: November 3, 2025

Correspondence
Trong Binh Le, MD, PhD
Department of Radiology,
Hue University of Medicine and Pharmacy, Hue University,
06 Ngo Quyen, Hue 530000,
Vietnam.
E-mail: letrongbinh@hueuni.edu.vn

Benign Versus Malignant Solid Liver Lesions: How Can Apparent Diffusion Coefficient Value Be Added to the Differentiation?

Hong Phuong Dung Tran[1], Ngoc Thanh Hoang[1,2], Cam Nhung Dang[1], Thanh Thao Nguyen[1], and Trong Binh Le[1]

[1]Department of Radiology, Hue University of Medicine and Pharmacy, Hue University, Hue, Vietnam
[2]Department of Radiological Sciences, Tokyo Metropolitan University, Tokyo, Japan

Purpose: To determine the efficacy of apparent diffusion coefficient (ADC) values and ratios (lesion/liver tissue, lesion/splenic tissue, lesion/paraspinal muscle) in differentiating benign from malignant solid liver lesions.

Materials and Methods: This study retrospectively analyzed data from 115 patients with solid liver lesions who underwent abdominal magnetic resonance imaging (MRI) at a single institution between January 2023 and December 2024. Lesions were classified as benign or malignant based on biochemical tests as well as radiographic and/or histopathologic findings. ADC values and ratios were determined using a 1.5 T MRI scanner. Quantitative variables are presented as mean ± standard deviation or median (interquartile range). Receiver operating characteristic (ROC) analysis was used to determine the cut-off values for ADC value and ratio, for which associated areas under the ROC curve were calculated.

Results: The present analysis included 115 lesions—36 benign and 79 malignant. The median ADC value of the benign lesions was significantly higher than that of malignant lesions: 1744.5 × 10^{-6} mm^2/s vs. 1168.0 × 10^{-6} mm^2/s, respectively. The average lesion-to-liver ADC ($rADC_l$), lesion-to-spleen ADC ($rADC_{sp}$), and lesion-to-paraspinal muscle ADC ($rADC_m$) ratios for the benign lesions were significantly higher than those of malignant lesions: 1.79 vs. 1.09, 2.31 vs. 1.44, and 1.19 vs 0.80, respectively. A threshold of 1416 × 10^{-6} mm^2/s was used to differentiate benign vs. malignant lesions, with a sensitivity of 83.3% and a specificity of 78.5%. The cut-off values for $rADC_l$, $rADC_{sp}$, and $rADC_m$ were 1.55, 1.95, and 0.97, respectively, with sensitivities of 69.4%, 69.4%, and 83.3% and specificities of 87.3%, 91.1%, and 79.9%, respectively.

Conclusion: ADC metrics obtained from diffusion-weighted MRI effectively distinguished benign from malignant solid liver lesions.

Keywords: Diffusion-weighted imaging; Apparent diffusion coefficient; Apparent diffusion coefficient ratio; Liver lesion, benign, malignant

INTRODUCTION

The accurate classification of focal liver lesions is crucial for management planning and selecting the optimal therapeutic approach. Magnetic resonance imaging (MRI) has been proven superior to computed tomography in detecting and characterizing such lesions, owing to the diversity and specificity of the various available sequences [1]. One such sequence, diffusion-weighted imaging (DWI), is a noninvasive and non-contrast-enhanced sequence widely used in the diagnosis of hepatic disorders. The mechanism of DWI is based on the Brownian motion of water molecules within a tissue voxel, which provides data on quantitative tissue cellularity, viscosity, and extracellular space and depicts the relationship between normal and malignant tissues [2,3]. The magnitude of diffusion within the tissue displayed can be quantitatively measured from the DWI apparent diffusion coefficient (ADC) map [1,4].

In addition to its applications in stroke imaging, DWI, which was first used for tumor characterization in brain tumors [3], provides quantitative and qualitative information on unique tumor characteristics, evolution, and treatment response assessment. Tumors are often more densely cellular than normal tissue, resulting in restricted diffusion (high signal on DWI). Malignant lesions exhibit lower ADC values owing to the following factors: increased cell density, disrupted tissue structure, and increased extracellular space tortuosity, all of which reduce the motion of water [3,5]. While ADC values have shown considerable promise in improving the non-invasive characterization of liver lesions, their diagnostic performance has not yet been elucidated. In fact, there have been conflicting studies regarding the efficacy of ADC in discriminating malignant from benign focal liver lesions. While some studies observed statistically significant differences in ADC between malignant and benign lesions [1,6], others found that using ADC for this task is unreliable due to the substantial overlap of ADC values [7,8]. ADC values in the same lesion can vary based on the MRI scanner, protocol, and analysis software platform used [9]. The values within a particular lesion can even vary during separate examinations owing to variations in biological factors such as vascularity and membrane permeability changes. As such, studies aiming to enhance the diagnostic accuracy and robustness of DWI-based assessments are ongoing. Fortunately, normalizing the ADC value of a lesion to that of a reference tissue, such as the adjacent normal liver parenchyma, splenic tissue, or paraspinal muscle, can overcome the aforementioned limitations and provide a more reliable depiction of diffusion changes relative to normal tissue [10,11].

This study aimed to assess the efficacy of using ADC values of liver lesions and ADC value ratios (lesion/liver tissue, lesion/splenic tissue, lesion/paraspinal muscle) in differentiating benign from malignant liver lesions.

MATERIALS AND METHODS

Study Population

The protocol for this study was approved by the institutional review board of Hue University of Medicine and Pharmacy (number 01/22) and informed consent was obtained from all patients.

This retrospective study involved a cross-sectional analysis of 115 patients with focal liver lesions who underwent abdominal MRI between January 2023 and March 2024 at our institution. All patients ≥18 years of age who had at least one hepatic lesion >10 mm in maximal diameter were included in this analysis. The exclusion criteria were as follows: ongoing chemotherapy, history of liver resection or splenectomy, and MRI contraindicated. Patients with simple hepatic cysts were also excluded from the analysis.

Based on imaging findings as well as biochemical and/or histologic test results, the target lesions were categorized into seven distinct types under two primary categories, as follows: benign (hemangioma, focal nodular hyperplasia [FNH], adenoma, and focal inflammatory lesion) and malignant (liver metastasis, intrahepatic cholangiocarcinoma [ICC], and hepatocellular carcinoma [HCC]).

Diagnostic Criteria

HCC was diagnosed based on the European Association for the Study of the Liver (EASL) 2018 practice guidelines, whereas ICC was confirmed histologically [12]. Liver metastasis was diagnoses based on imaging findings in the setting of known primary malignancy, with or without histopathologic confirmation. Metastases typically appear hypointense on non-contrast T1-weighted (T1W) and mildly-to-moderately hyperintense on T2-weighted (T2W) MRI sequences, with a frequent targetoid pattern on DWI. On contrast-enhanced MRI, enhancement behavior varies according to vascularity: hypovascular metastases typically show persistent hypoenhancement, while hypervascular lesions demonstrate peripheral rim enhancement during the arterial phase. This rim often reflects viable tumor tissue, with central non-enhancement indicating necrosis or cystic change—hallmarks of advanced metastatic progression [13,14]. Typical benign lesions were confirmed radiographically and diagnosed according to the EASL guidelines [15]. Other lesions were deemed benign if they remained stable in size on dynamic imaging follow-up obtained ≥6 months after the initial imaging; otherwise, percutaneous biopsy was required to confirm the diagnosis.

Liver MRI Protocol

Liver MRIs were performed on a 1.5 T MRI scanner (Amira; Siemens). A respiratory-triggered fat-suppressed single-shot echoplanar DWI sequence was obtained in the axial plane with three diffusion gradient directions. Table 1 shows the detailed parameters of this pulse sequence. Our institutional routine liver MRI protocol also included T2W single-shot fast spin echo axial/coronal, T2W fat sat axial, and gradient-recalled echo T1W in- and out-of-phase axial/coronal acquisitions before and after the injection of gadolinium.

Image Interpretation

All MRIs were performed by a senior radiologic technologist with >10 years of experience in MRI. Regions of interest (ROIs) were placed in target lesion, background liver, spleen, and paraspinal muscle tissues, avoiding cystic or necrotic appearing regions adjacent to the vessels. For lesions with a heterogeneous signal on DWI sequences, ROIs were placed at the most hypo- and hyperdense areas within the enhanced solid components. Conversely, for lesions with a homogeneous appearance, ROIs were placed at different axial slices within the lesion. The ADC values for each anatomic location were calculated as the average of the relevant ROIs, as follows: hepatic ADC values were derived from four ROIs placed in the lateral, medial, anterior, and posterior segments of the liver, while spleen and bilateral paraspinal muscle ADC values were derived from two ROIs placed in each structure. The average ADC value from all of the ROIs in each anatomic structure was used for the subsequent analysis. All ROI measurements had a 5–10-mm radius on DWI images, and parametric MRI (www.parametricmri.com) was used for image post-processing and analysis. ADC values were calculated based on linear and non-linear exponential fits. Two abdominal radiology fellows placed all of the ROIs and were responsible for verifying image quality and obtaining ADC value measurements. Two abdominal radiologists with >15 years of experience each were responsible for image analysis and interpretation, evaluating the contour, border, signal characteristics, and qualitative DWI features of the lesions.

Table 1. Diffusion-weighted imaging acquisition parameters

Parameters	Values
Repetition time (ms)	7900
Echo time (ms)	70
Base resolution	134
Field of view (mm)	380
Phase encoding direction	Anterior to posterior
Slice thickness (mm)	4.0
Distance factor (%)	20
b-values (s/mm^2)	50, 400, 800
Number of averages	b = 50 (1 average) b = 400 (3 averages) b = 800 (5 averages)
Fat suppression technique	Spectral Attenuated Inversion Recovery
Parallel imaging technique	Generalized autocalibrating partial (acceleration factor 2)
Scan time (min)	4

Statistics

Continuous data are presented as mean ± standard deviation if the variables were normally distributed, in which case Student's t-test was utilized to ascertain the difference between the independent samples (benign vs. malignant). If the variables were not normally distributed, however, the data are presented as median with interquartile range (IQR), and the Mann–Whitney U test was utilized accordingly. Categorical data are presented as counts and percentages. Levene's test was used to evaluate whether the variances across the ADC values of two or more groups were equal. The receiver operating characteristic (ROC) curve was analyzed to determine the cut-off threshold for the differential diagnosis of benign vs. malignant liver lesions, and the area under the ROC curve (AUC) was used to determine the threshold value, which was categorized as follows: excellent (≥90%), considerable (81%–90%), fair (71%–80%), poor (61%–70%), and fail (50%–60%) [16]. All analyses were performed using SPSS 20.0 (IBM Corp.) software. A p-value < 0.05 indicated statistical significance for all comparisons.

RESULTS

A total of 115 patients were included in the analysis. The median age was 56.2 ± 14.1 years (range, 25–89 years) and male/female ratio was 1.74. There were 36 benign and 79 malignant lesions, with an average maximal transverse diameter of 44.2 ± 31.4 mm (range, 12–165 mm). Table 2 summarizes the imaging characteristics of all of the lesions.

The median (IQR) ADC value across all lesions was 1280.0 (529) × 10^{-6} mm^2/s. The highest and lowest ADC values observed for hemangiomas (Fig. 1) and HCCs, at 3235 × 10^{-6} mm^2/s and 650 × 10^{-6} mm^2/s, respectively. The median (IQR) ADC value of the benign lesions was higher than that of the malignant lesions, at 1744.5 (818) × 10^{-6} mm^2/s and 1168.0 (387) × 10^{-6} mm^2/s, respectively ($p < 0.001$). Additionally, the benign lesions had higher average lesion-to-liver ADC ($rADC_l$), lesion-to-spleen ADC ($rADC_{sp}$), and lesion-to-paraspinal muscle ADC ($rADC_m$) ratios than the malignant lesions, at 1.79 vs. 1.09, 2.31 vs. 1.44, and 1.19 vs. 0.80, respectively ($p < 0.001$) (Table 3 and Fig. 2).

Table 2. Patient demographics and MRI morphological characteristics of all lesions

Parameters	Benign (n = 36)	Malignant (n = 79)	Total (n = 115)	p
Age (yr)	46.7 ± 13.6	60.5 ± 12.2	56.2 ± 14.1	
Sex				>0.05
Male	20 (17.4)	53 (46.1)	73 (63.5)	
Female	16 (13.9)	26 (22.6)	42 (36.5)	
Transverse diameter (mm)	32.9 ± 18.5	49.4 ± 34.6	44.2 ± 31.4	
Outer contour				>0.05
Regular	21 (18.3)	46 (40.0)	67 (58.3)	
Irregular	15 (13.0)	33 (28.7)	48 (41.7)	
Border				>0.05
Well-defined	35 (30.4)	74 (64.4)	109 (94.8)	
Poorly defined	1 (0.9)	5 (4.3)	6 (5.2)	
Signal intensity pattern				<0.05
Homogeneous	24 (20.9)	33 (24.7)	57 (49.6)	
Heterogeneous	12 (10.4)	46 (40.0)	58 (50.4)	
T1W				>0.05
Hyperintense	3 (2.6)	3 (2.6)	6 (5.2)	
Hypointense	28 (24.3)	70 (60.9)	98 (85.2)	
Isointense	5 (4.3)	6 (5.3)	11 (9.6)	
T2W				>0.05
Hyperintense	32 (27.8)	68 (59.1)	100 (87.0)	
Hypointense	1 (0.9)	3 (2.6)	4 (3.5)	
Isointense	3 (2.6)	8 (7.0)	11 (9.6)	
DWI				>0.05
Hyperintense	33 (28.7)	74 (64.3)	107 (93.0)	
Hypointense	0 (0)	1 (0.9)	1 (0.9)	
Isointense	3 (2.6)	4 (3.5)	7 (6.1)	

Values are presented as mean ± standard deviation or number (%).
*p-values show a significant difference between two groups.
T1W, T1-weighted; T2W, T2-weighted; DWI, diffusion-weighted imaging.

The diagnostic thresholds for differentiating benign from malignant lesions were as follows: ADC value, 1416 × 10^{-6} mm^2/s (sensitivity, 83.3%; specificity, 78.5%; AUC, 84.5%); $rADC_l$ ratio, 1.55 (sensitivity, 69.4%; specificity, 87.3%; AUC, 82.5%); $rADC_{sp}$ ratio, 1.95 (sensitivity, 69.4%; specificity, 91.1%; AUC, 85.0%); and $rADC_m$ ratio, 0.97 (sensitivity, 83.3%; specificity, 79.9%; AUC, 84.4%) (Fig. 3).

DISCUSSION

The results of the present study demonstrated that ADC quantification was effective in differentiating benign from malignant liver lesions. Previous studies have proposed a range of ADC thresholds, largely owing to the various parameters used to obtain ADC maps and the measurement techniques involved. Additionally, the accuracy of lesion detection and characterization varies depending on the patient population and lesion type [9]. However, it has been generally acknowledged that benign liver lesions have higher ADC values than their malignant counterparts, despite the significant overlap for specific lesions [6,17]. Cell density is an essential histologic feature that substantiates the use of ADC values to differentiate benign from malignant lesions. Theoretically, water molecules can move more freely in structures with a lower cell density, resulting in a less progressive signal with increased b-values, which corresponds to high ADC values that are often associated with benign lesions. Meanwhile, dense cellularity is a hallmark of aggressive malignancies (Fig. 4), such as HCC, ICC, and metastasis, indicative of rapid proliferation and invasion into surrounding tissues, often with little-to-no surrounding stroma [18,19].

The disparity among ADC value cut-offs can be explained by the different imaging techniques (such as the choice of b-values and other acquisition parameters) and MRI scanners utilized in clinical practice. ADC values may exhibit up to 10% inter-center variability, primarily attributable to differences in DWI sequence parameters [20]. In one study, when obtaining MRIs with identical parameters on the same group of patients, separated by a 15-min interval, the ADC value in liver tumors can varied by up to 30% between the two scans [21].

Prior studies have highlighted significant discrepancies in ADC values between abdominal tumors and adjacent normal tissues. Consequently, normalized ADC values are considered more robust than raw measurements to reduce the variability in ADC value calculations. Both the spleen and paraspinal muscles have been proposed as potential reference tissues, as while hepatic parenchymal ADC values are influenced by sex, age, and iron overload, splenic ADC values remain consistent and are minimally influenced by patient-related factors or concomitant liver pathologies [22]. Paraspinal muscle tissue, however, has demonstrated greater stability, supporting its role as a more reliable internal reference for the differentiation of benign from malignant tumors on abdominal imaging [20,23]. Therefore, in this study we used the ADC ratio analysis method to minimize heterogeneity caused by these confounding factors. $rADC_l$, $rADC_{sp}$, and $rADC_m$ are easily calculated and can be readily applied without requiring designated software or formulas. These ratios have been proven to neutralize potential confounding factors, allowing for an accurate differentiation between lesions [10,22].

The findings of the present study are in agreement with previously published data. Benign lesions had significantly higher ADC values than malignant lesions. Of note, hemangiomas had the highest ADC value (3235 × 10^{-6} mm^2/s) among the lesions evaluated. We also established a cut-off point of 1416 × 10^{-6}

mm^2/s to differentiate between benign and malignant hepatic lesions, with a sensitivity of 83.3%, specificity of 78.5%, and AUC of 84.5%. Furthermore, the average $rADC_l$, $rADC_{sp}$, and $rADC_m$ were significantly higher for benign than malignant lesions. The optimal cut-off values for $rADC_l$, $rADC_{sp}$, and $rADC_m$ to differentiate between benign and malignant lesions were 1.55, 1.95, and 0.97 respectively, with sensitivities of 69.4%, 69.4%, and 83.3%; specificities of 87.3%, 91.1%, and 79.7%; and AUCs of 82.5%, 85.0%, and 84.4%, respectively. These cut-off thresholds demonstrated considerable AUCs, ranging between 80% and 90%, indicating good diagnostic performance. Relative ADC values typically exhibit greater specificity than

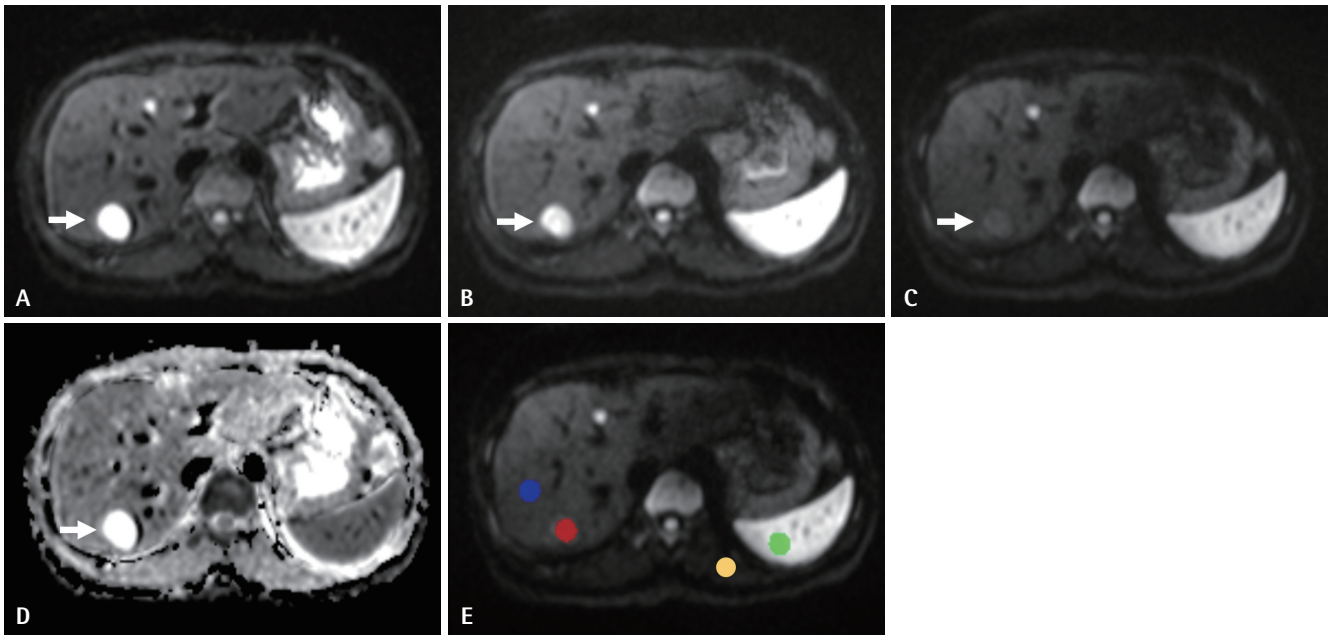

Fig. 1. Apparent diffusion coefficient (ADC) quantification of a hepatic hemangioma. A–C: The tumor (arrow) demonstrates high signal intensity on diffusion-weighted imaging (DWI) at a b-value of 50, with a decrease in intensity at b-values of 400 and 800, respectively. D: Medium-to-high signal intensity was observed on the ADC map, consistent with no restricted diffusion. E: The tumor has a heterogeneous signal on DWI images, regions of interest (ROIs) were positioned at the most hypo- and hyperintense areas within the enhanced solid components. The tumor (red ROI) ADC value and lesion-to-liver (blue ROI), lesion-to-spleen (green ROI), lesion-to-muscle (yellow ROI) ADC ratios are 2486 × 10^{-6} mm^2/s, 2.23, 2.52, and 1.56, respectively. Dynamic enhancement was typical for hemangiomas. The lesion remained stable in size and enhancement pattern at the 1-year follow-up.

Table 3. ADC parameters and ADC ratios of all lesions

Type of lesion	n (%)	ADC value (×10^{-6} mm^2/s)		$rADC_l$ (lesion/liver)		$rADC_{sp}$ (lesion/spleen)		$rADC_m$ (lesion/muscle)	
		Median (IQR)	Mean ± SD	Median (IQR)	Mean ± SD	Median (IQR)	Mean ± SD	Median (IQR)	Mean ± SD
Benign lesion	36 (29)	1744.5 (818)	1821.1 ± 525	1.79 (0.93)	1.85 ± 0.63	2.31 (1.15)	2.36 ± 0.71	1.19 (0.56)	1.24 ± 0.36
Hemangioma	25 (21.7)	1896 (738)	2036.6 ± 452	1.92 (0.82)	2.03 ± 0.52	2.71 (0.94)	2.59 ± 0.62	1.33 (0.47)	1.38 ± 0.31
Adenoma	1 (0.9)	1339	1339	1.25	1.25	1.71	1.71	0.83	0.83
FNH	6 (5.2)	1294.5 (184)	1383.0 ± 186	1.17 (0.31)	1.30 ± 0.24	1.60 (0.37)	1.83 ± 0.37	0.90 (0.16)	0.94 ± 0.16
Inflammatory lesion	4 (3.4)	1414.5 (462)	891.3 ± 270	1.57 (1.71)	1.80 ± 0.92	1.68 (1.09)	1.80 ± 0.49	1.02 (0.33)	1.03 ± 0.18
Malignant lesion	79 (71)	1168.0 (387)	1258.6 ± 372	1.09 (0.41)	1.19 ± 0.37	1.44 (0.54)	1.55 ± 0.42	0.80 (0.24)	0.86 ± 0.24
HCC	49 (42.6)	1174.0 (343)	1206.4 ± 273	1.07 (0.42)	1.14 ± 0.30	1.39 (0.48)	1.51 ± 0.36	0.79 (0.23)	0.83 ± 0.18
Cholangiocarcinoma	10 (8.7)	1175.5 (446)	1259.2 ± 238	1.05 (0.46)	1.16 ± 0.26	1.72 (0.64)	1.64 ± 0.37	0.81 (0.31)	0.83 ± 0.16
Metastasis	19 (16.5)	1168.0 (502)	1141.2 ± 75	1.16 (0.65)	1.22 ± 0.38	1.45 (0.65)	1.54 ± 0.32	0.81 (0.27)	0.86 ± 0.20
Hepatoblastoma	1 (0.9)	1004		1.0	1.0	1.29	1.29	0.71	0.71
p		<0.001*		<0.001*		<0.001*		<0.001*	
Total	115 (100)	1280.0 (529)	1424.8 ± 496	1.25 (0.67)	1.38 ± 0.55	1.63 (0.69)	1.79 ± 0.64	0.87 (0.41)	0.97 ± 0.32

*p-values show a significant difference in ADC values and ratios of ADC between benign and malignant lesions (Mann–Whitney U test).
ADC, apparent diffusion coefficient; IQR, interquartile range; SD, standard deviation; $rADC_l$, lesion-to-liver ADC; $rADC_{sp}$, lesion-to-spleen ADC; $rADC_m$, lesion-to-paraspinal muscle ADC; FNH, focal nodular hyperplasia; HCC, hepatocellular carcinoma.

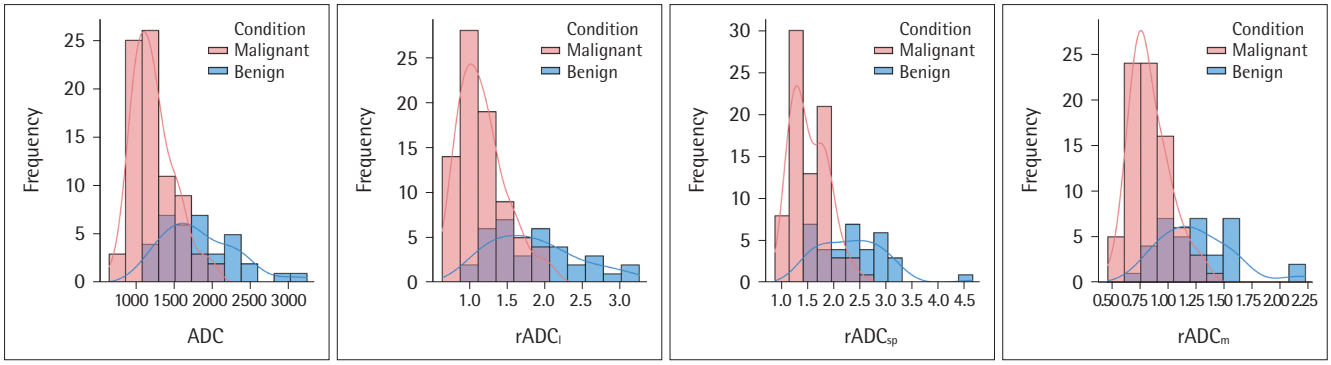

Fig. 2. Histogram and overlap of ADC values and ratios by lesion type (benign vs. malignant). The ADC value and lesion-to-liver ADC ($rADC_l$), lesion-to-spleen ADC ($rADC_{sp}$), and lesion-to-muscle ADC ($rADC_m$) ratios, respectively.

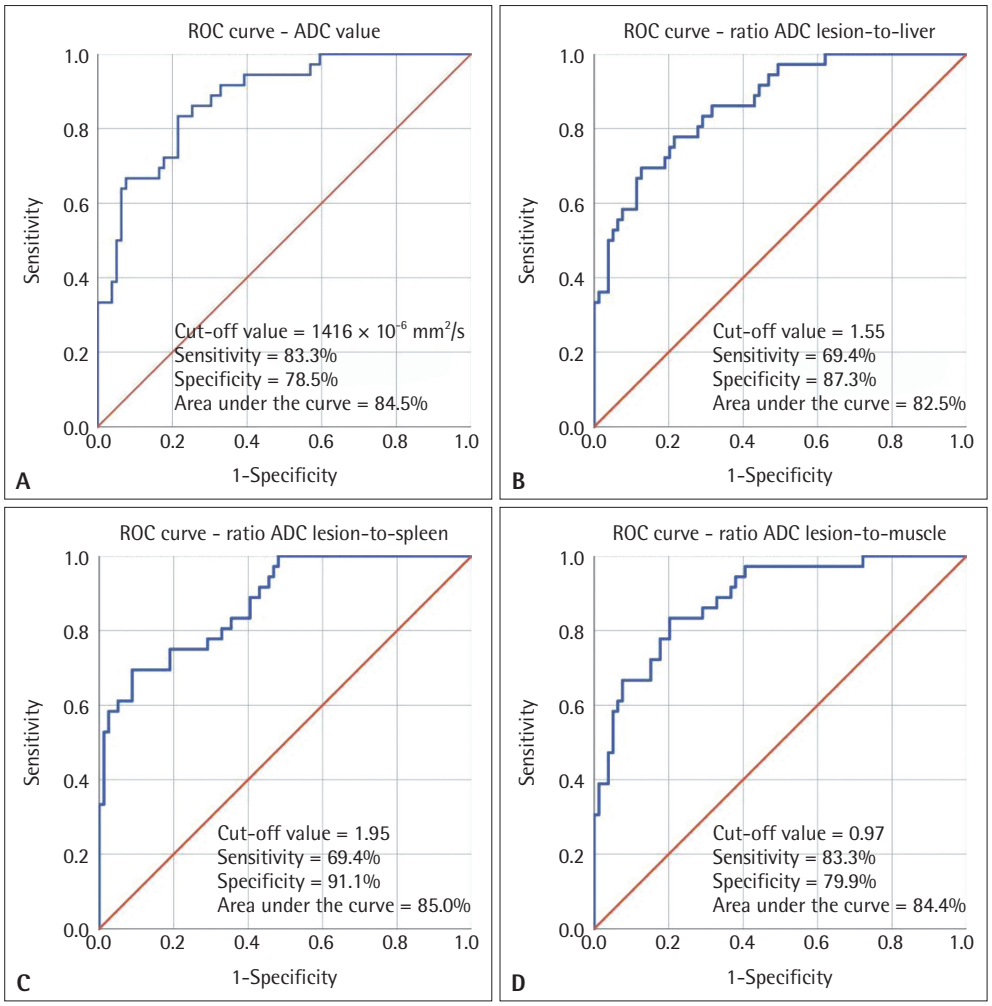

Fig. 3. Receiver operating characteristic (ROC) analysis of apparent diffusion coefficient (ADC) values, lesion-to-liver ADC ($rADC_l$), lesion-to-spleen ADC ($rADC_{sp}$), and lesion-to-muscle ADC ($rADC_m$). A: The cut-off ADC value for differentiating benign from malignant lesions is 1416 × 10^{-6} mm^2/s, with a sensitivity of 83.3%, specificity of 78.5%, and area under the ROC curve (AUC) of 84.5%. B: The optimal cut-off value for $rADC_l$ is 1.55, with a sensitivity of 69.4%, specificity of 87.3%, and AUC of 82.5%. C: The optimal cut-off value for $rADC_{sp}$ is 1.95, with a sensitivity of 69.4%, specificity of 91.1%, and AUC of 85.0%. D: The cut-off value for $rADC_m$ is 0.97, with a sensitivity of 83.3%, specificity of 79.9%, and AUC of 84.4%.

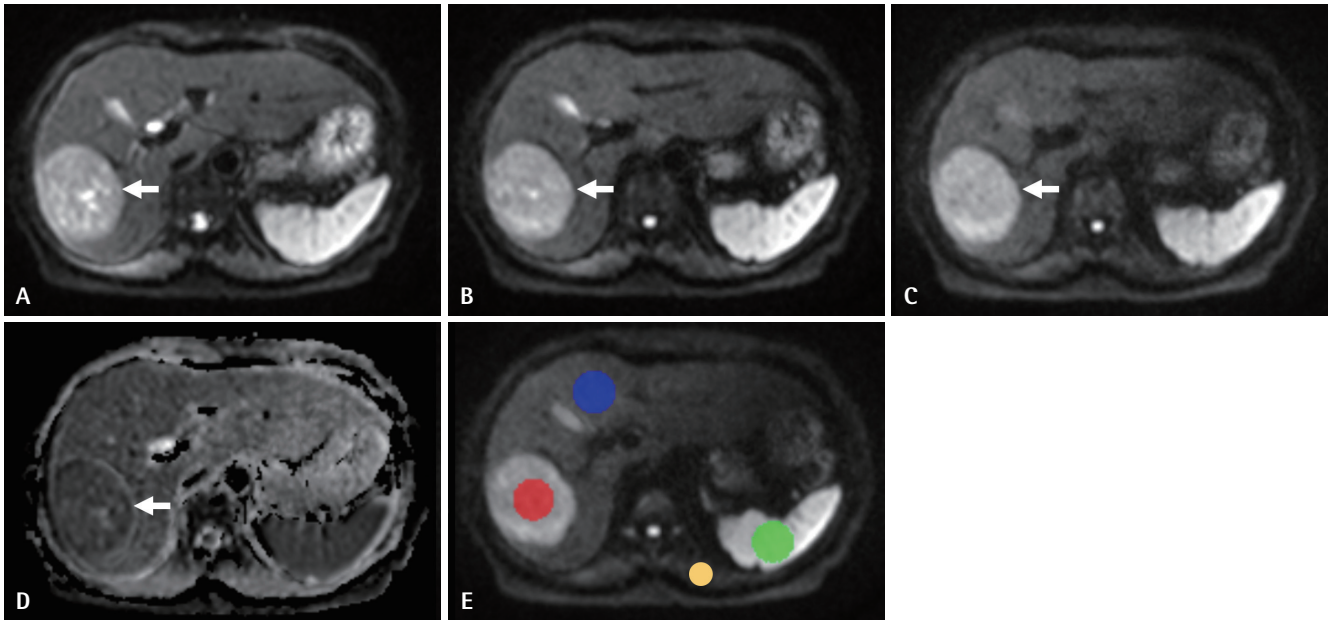

Fig. 4. Apparent diffusion coefficient (ADC) quantification of a pathologically confirmed hepatocellular carcinoma. A–C: The tumor (arrow) shows markedly increased signal intensity on diffusion-weighted imaging at b-values of 50, 400, and 800, respectively. D: Decreased signal intensity is observed on the ADC map, consistent with restricted diffusion. E: Regions of interest (ROIs) were placed in different axial slices within the lesion. The tumor ADC (red ROI), lesion-to-liver (blue ROI), lesion-to-spleen (green ROI), and lesion-to-muscle (yellow ROI) ADC values are 935 × 10^{-6} mm^2/s, 0.91, 1.17, and 0.65, respectively.

ADC values, with $rADC_{sp}$ showing the highest specificity among all of the ratios evaluated.

Several previous studies have explored the role of ADC and rADC values in the diagnostic process. A meta-analysis of 14 prior studies found that ADC threshold values for differentiating malignant from benign solid liver lesions varied from 810 to 1600 × 10^{-6} mm^2/s, with a pooled sensitivity of 78%, pooled specificity of 74%, and AUC of 82% [6]. Gelebek Yılmaz and Yıldırım [24] reported that a cut-off ADC value of 1260 × 10^{-6} mm^2/s and ADC ratio of 0.90 were useful in distinguishing benign from malignant lesions, with sensitivities of 92% and 85% and specificities of 94% and 92%, respectively. Additionally, the ADC ratio of benign lesions was 1.50 ± 0.53, significantly higher than that of malignant lesions, which was 0.80 ± 0.20. They also speculated that the ADC ratio for lesion/liver parenchyma achieved higher diagnostic accuracy in differentiating metastases from benign solid lesions than the ADC value alone [24]. Another study, which included 39 benign and 36 malignant lesions, documented an ADC value of 1260 × 10^{-6} mm^2/s and ADC ratio for lesion/liver of 1.1 as the optimal cut-off values, with sensitivities of 92% and 82%, specificities of 80% and 86%, and overall accuracies of 89% and 92%, respectively [10]. Sharma et al. [25] proposed that malignant lesions had a mean ADC of 1130 × 10^{-6} mm^2/s, while that for benign lesions was 1630 × 10^{-6} mm^2/s. They also found that a threshold of 1350 × 10^{-6} mm^2/s served as an adjunct to other MRI parameters for characterizing focal liver lesions as either benign or malignant, achieving a sensitivity of 85.7%, specificity of 88%, positive predictive value of 88%, and negative predictive value of 85.7%. Jahic et al. [26] reported average ADC values of 1880 (range, 1326–2480) × 10^{-6} mm^2/s for benign lesions, and 1150 (range, 1024–1343) × 10^{-6} mm^2/s for malignant lesions, with a cut-off value of 1341 × 10^{-6} mm^2/s. Caraiani et al. [1] further emphasized that decreased ADC values and ratios (compared to liver parenchyma) were an accurate method for differentiating benign from malignant lesions. Most of the proposed thresholds are close to the upper limit of 1600 × 10^{-6} mm^2/s, similar to our results. Therefore, further investigation with a larger population is warranted to narrow this cut-off range.

One study showed that the renal medulla was an effective reference organ—the ADC ratio for liver lesions aided in differential diagnosis with high sensitivity (95%) and specificity (72%) [27]. Occasionally, ADC values can be utilized in the differential diagnosis of some specific lesions [17]. Thanks to their remarkably high ADC values, atypical hemangiomas can be differentiated from malignant lesions when signal intensity and enhancement characteristics are otherwise inconclusive.

Additionally, the differentiation of smaller lesions can present a challenge, owing to partial volume effects and less-than-ideal ROI measurements, potentially skewing ADC values. Although ADC quantification appears useful in distinguishing benign from malignant solid hepatic lesions, further categorization into specific entities is unreliable since current data

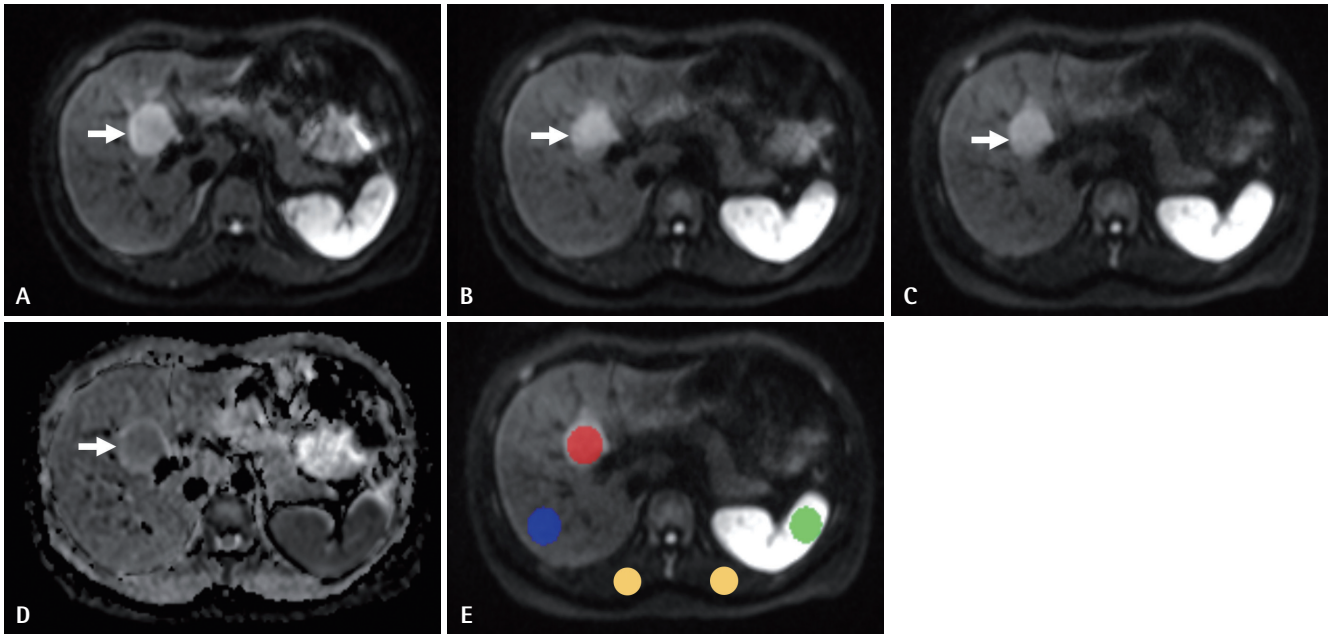

Fig. 5. Apparent diffusion coefficient (ADC) quantification of a pathologically confirmed hepatic adenoma. A–C: The tumor (arrow) shows increased signal intensity on diffusion-weighted imaging at b-values of 50, 400, and 800, respectively. D: Intermediate signal intensity was observed on the ADC map. E: Regions of interest were placed at three different anatomic locations: within the lesion (red), liver parenchyma (blue), spleen (green), and paraspinal muscle (yellow). The tumor ADC value and lesion-to-liver ADC, lesionto-spleen ADC, and lesion-to-paraspinal muscle ADC are 1339 × 10^{-6} mm^2/s, 1.25, 1.71, and 0.83, respectively.

are scarce and heterogeneous. Radiographically, some benign lesions (adenomas, FNHs) might exhibit restricted diffusion (Fig. 5), similar to that of malignant lesions (HCCs, ICCs, metastases) owing to their cell-rich nature [17,19]. Conversely, malignant lesions with cystic necrosis can have decreased ADC values [10,17], representing a critical limitation of using absolute ADC values alone for characterizing hepatic lesions. At present, therefore, ADC values provide supplementary diagnostic information alongside conventional imaging characteristics.

There are some limitations of this study, which include: small sample size, single institution, and the fact that some of the lesions were not confirmed pathologically. Therefore, future studies would benefit from including a larger study population.

In conclusion, benign solid liver lesions have significantly higher ADC values (threshold, 1416 × 10^{-6} mm^2/s), $rADC_l$ ratio (cut-off, 1.55), $rADC_{sp}$ ratio (cut-off, 1.95), and $rADC_m$ ratio (cut-off, 0.97) than malignant lesions. Both ADC value and ratio are effective in distinguishing benign from malignant lesions, with the lesion-to-spleen and lesion-to-paraspinal muscle ADC ratios showing the best specificity.

Availability of Data and Material

The datasets generated or analyzed during the study are available from the corresponding author on reasonable request.

Conflicts of Interest

The authors have no potential conflicts of interest to disclose.

Author Contributions

Conceptualization: Hong Phuong Dung Tran, Ngoc Thanh Hoang. Data curation: Hong Phuong Dung Tran, Cam Nhung Dang. Formal analysis: Hong Phuong Dung Tran, Ngoc Thanh Hoang. Funding acquisition: Thanh Thao Nguyen, Trong Binh Le. Investigation: Hong Phuong Dung Tran, Ngoc Thanh Hoang. Methodology: Hong Phuong Dung Tran, Ngoc Thanh Hoang. Project administration: Hong Phuong Dung Tran, Thanh Thao Nguyen. Resources: Hong Phuong Dung Tran. Software: Hong Phuong Dung Tran, Ngoc Thanh Hoang. Supervision: Thanh Thao Nguyen, Trong Binh Le. Validation: Thanh Thao Nguyen, Trong Binh Le. Visualization: Hong Phuong Dung Tran, Ngoc Thanh Hoang. Writing—original draft: Hong Phuong Dung Tran, Ngoc Thanh Hoang, Cam Nhung Dang. Writing—review & editing: all authors.

ORCID iDs

Hong Phuong Dung Tran https://orcid.org/0000-0002-8766-4306
Ngoc Thanh Hoang https://orcid.org/0000-0002-9498-464X
Cam Nhung Dang https://orcid.org/0009-0000-6300-2634
Thanh Thao Nguyen https://orcid.org/0000-0001-9379-6359
Trong Binh Le https://orcid.org/0000-0001-5444-5708

Funding Statement

This study was supported by Hue University under the Core Research Program, Grant No. NCM.DHH.2020.09.

Acknowledgments

None

REFERENCES

1. Caraiani C, Chiorean L, Fenesan DI, et al. Diffusion weighted magnetic resonance imaging for the classification of focal liver lesions as benign or malignant. J Gastrointestin Liver Dis 2015; 24:309-317.
2. Bammer R. Basic principles of diffusion-weighted imaging. Eur J Radiol 2003;45:169-184.
3. Koh DM, Collins DJ. Diffusion-weighted MRI in the body: applications and challenges in oncology. AJR Am J Roentgenol 2007; 188:1622-1635.
4. Testa ML, Chojniak R, Sene LS, et al. Is DWI/ADC a useful tool in the characterization of focal hepatic lesions suspected of malignancy? PLoS One 2014;9:e101944.
5. Kamel IR, Liapi E, Reyes DK, Zahurak M, Bluemke DA, Geschwind JF. Unresectable hepatocellular carcinoma: serial early vascular and cellular changes after transarterial chemoembolization as detected with MR imaging. Radiology 2009;250:466-473.
6. Nalaini F, Shahbazi F, Mousavinezhad SM, Ansari A, Salehi M. Diagnostic accuracy of apparent diffusion coefficient (ADC) value in differentiating malignant from benign solid liver lesions: a systematic review and meta-analysis. Br J Radiol 2021;94: 20210059.
7. Filipe JP, Curvo-Semedo L, Casalta-Lopes J, Marques MC, Caseiro-Alves F. Diffusion-weighted imaging of the liver: usefulness of ADC values in the differential diagnosis of focal lesions and effect of ROI methods on ADC measurements. MAGMA 2013;26: 303-312.
8. Sutherland T, Steele E, van Tonder F, Yap K. Solid focal liver lesion characterisation with apparent diffusion coefficient ratios. J Med Imaging Radiat Oncol 2014;58:32-37.
9. Culverwell AD, Sheridan MB, Guthrie JA, Scarsbrook AF. Diffusion-weighted MRI of the liver-Interpretative pearls and pitfalls. Clin Radiol 2013;68:406-414.
10. Pankaj Jain T, Kan WT, Edward S, Fernon H, Kansan Naider R. Evaluation of ADCratio on liver MRI diffusion to discriminate benign versus malignant solid liver lesions. Eur J Radiol Open 2018;5:209-214.
11. Colagrande S, Regini F, Pasquinelli F, et al. Focal liver lesion classification and characterization in noncirrhotic liver: a prospective comparison of diffusion-weighted magnetic resonance-related parameters. J Comput Assist Tomogr 2013;37:560-567.
12. European Association for the Study of the Liver. EASL clinical practice guidelines on the management of hepatic encephalopathy. J Hepatol 2022;77:807-824.
13. Ozaki K, Higuchi S, Kimura H, Gabata T. Liver metastases: correlation between imaging features and pathomolecular environments. Radiographics 2022;42:1994-2013.
14. Maino C, Vernuccio F, Cannella R, et al. Liver metastases: the role of magnetic resonance imaging. World J Gastroenterol 2023; 29:5180-5197.
15. European Association for the Study of the Liver (EASL). EASL clinical practice guidelines on the management of benign liver tumours. J Hepatol 2016;65:386-398.
16. Çorbacıoğlu ŞK, Aksel G. Receiver operating characteristic curve analysis in diagnostic accuracy studies: a guide to interpreting the area under the curve value. Turk J Emerg Med 2023;23:195-198.
17. Tanyerı A, Cıldag MB, Koseoglu OFK. Effectiveness of ADC histogram analysis in the diagnosis of focal liver lesions; is a contrast agent necessary? Marmara Med J 2022;35:187-195.
18. Crowe PM, Olliff JF. MRI of focal liver lesions. Imaging 1998;10: 59-72.
19. Vallejo Desviat P, Martínez De Vega V, Recio Rodríguez M, Jiménez De La Peña M, Carrascoso Arranz J. [Diffusion MRI in the study of hepatic lesions]. Cir Esp 2013;91:9-16. Spanish
20. Chen Y, Yang P, Fu C, et al. Variabilities in apparent diffusion coefficient (ADC) measurements of the spleen and the paraspinal muscle: a single center large cohort study. Heliyon 2023;9: e18166.
21. Kim SY, Lee SS, Byun JH, et al. Malignant hepatic tumors: short-term reproducibility of apparent diffusion coefficients with breath-hold and respiratory-triggered diffusion-weighted MR imaging. Radiology 2010;255:815-823.
22. El-Hariri M, Ali TFT, Hussien HI. Apparent diffusion coefficient (ADC) in liver fibrosis: usefulness of normalized ADC using the spleen as reference organ. Egypti J Radiol Nucl Med 2013;44: 441-451.
23. Michoux NF, Ceranka JW, Vandemeulebroucke J, et al. Repeatability and reproducibility of ADC measurements: a prospective multicenter whole-body-MRI study. Eur Radiol 2021;31:4514-4527.
24. Gelebek Yılmaz F, Yıldırım AE. Relative contribution of apparent diffusion coefficient (ADC) values and ADC ratios of focal hepatic lesions in the characterization of benign and malignant lesions. Eur J Ther 2018;24:150-157.
25. Sharma S, Dalal V, Prem Kumar G, Malhotra P. Diffusion MRI with quantification of ADC value in characterization of benign and malignant hepatic lesions and their correlation with cytohistopathology. IP Int J Med Paediatr Oncol 2020;6:131-135.
26. Jahic E, Sofic A, Selimovic AH. DWI/ADC in differentiation of benign from malignant focal liver lesion. Acta Inform Med 2016; 24:244-247.
27. Uçar N, Karakaş L, Yılmaz E, Ekin EE, Bayrak AH, Özkurt H. Utility of relative ADC in discriminating the benign and malign liver masses: diagnostic potential in comparison to ADC. J Acad Res Med 2024;14:40-47.